Article

In Vivo Molecular Insights into Syntrophic Geobacter Aggregates

Wenchao Wei, Andrew E. Plymale, Zihua Zhu, Xiang Ma, Fanghua Liu, and Xiao-Ying Yu

Anal. Chem., **Just Accepted Manuscript** • DOI: 10.1021/acs.analchem.0c00653 • Publication Date (Web): 02 Jul 2020

In Vivo Molecular Insights into Syntrophic *Geobacter* Aggregates

Wenchao Wei,[†,§,≠] Andrew Plymale,[§] Zihua Zhu,[‡] Xiang Ma,[⊥] Fanghua Liu,[†,*] and Xiao-Ying Yu[§,*]

[†]Key Laboratory of Coastal Biology and Utilization, Yantai Institute of Coastal Zone Research, Chinese Academy of Sciences, Yantai, Shandong 264003, China

[§]Energy and Environment Directorate, Pacific Northwest National Laboratory, Richland, Washington 99352, United States

[≠]University of Chinese Academy of Sciences, Beijing 100049, China

[⊥]Department of Chemistry, Grand View University, Des Moines, Iowa 50316, United States

[‡]Environmental and Molecular Science Laboratory, Pacific Northwest National Laboratory, Richland, Washington 99352, United States

*E-mail: xiaoying.yu@pnnl.gov; fhliu@yic.ac.cn

Supporting Information Placeholder

ABSTRACT: Direct interspecies electron transfer (DIET) has been considered as a novel and highly efficient strategy in both natural anaerobic environments and artificial microbial fuel cells. A syntrophic model consisting of *Geobacter metallireducens* and *Geobacter sulfurreducens* was studied in this work. We conducted *in vivo* molecular mapping of the outer surface of the syntrophic community as the interface of nutrients and energy exchange. System for Analysis at the Liquid Vacuum Interface (SALVI) combined with time-of-flight secondary ion mass spectrometry (ToF-SIMS) was employed to capture the molecular distribution of syntrophic *Geobacter* communities in the living and hydrated state. Principal component analysis (PCA) with selected peaks revealed that syntrophic *Geobacter* aggregates were well differentiated from other control samples, including syntrophic planktonic cells, pure cultured planktonic cells, and single population biofilms. Our *in vivo* imaging indicated that a unique molecular surface was formed. Specifically, aromatic amino acids, phosphatidylethanolamine (PE) components, and large water clusters were identified as key components that favored the DIET of syntrophic *Geobacter* aggregates. Moreover, the molecular changes in depths of the *Geobacter* aggregates were captured using dynamic depth profiling. Our findings shed new light on the interface components supporting electron transfer in syntrophic communities based on *in vivo* molecular imaging.

Introduction

In the past decade, direct interspecies electron transfer (DIET) has been demonstrated as a novel and highly efficient microbial energy strategy in anaerobic environments such as wetlands, ocean sediments, and sewage treatment plants. DIET not only occurs in bacteria-to-bacteria but also bacteria to archaea.[1-3] Notably, the formation of syntrophic aggregates or consortia was often accompanied.[4, 5] One of the best known models is the well-defined co-cultured aggregates formed by *Geobacter metallireducens* (GS15) and *Geobacter sulfurreducens* (DL1). In this co-culture, ethanol is the sole exogenous electron donor, and can only be used by *G. metallireducens*; and fumarate is the sole exogenous electron acceptor and can only be used by *G. sulfurreducens*.[4] To better understand the mechanism of how syntrophic *Geobacter* species build their communities, the outer surface, which is the most active layer and plays an important role in the exchange of nutrients and wastes, as well as the recruitment of new members, warrants more investigations.

Although intense studies have been done in the illustration of the role of extracellular c-type cytochromes and pili,[6-10] knowledge of other potentially cardinal molecules is limited. While proteomic analysis using LC-MS/MS could provide a global view of protein changes,[11] the results were derived from the bulk instead of the biointerface of interest in this work. At this point, information from molecular mapping of the syntrophic community surface is needed, which could provide new mechanistic insights into DIET. Recently, the atomic distribution of pure cultured *Geobacter sulfurreducens* has been characterized by the combination of energy dispersive X-ray spectroscopy (EDXS) and high annular dark field (HAADF).[12] Molecular information of syntrophic *Geobacter* communities has also been characterized by static time-of-flight secondary ion spectrometry (ToF-SIMS) using dried samples.[13] Although both approaches show promises in DIET, static SIMS is limited to dry solid samples. Drying and freezing of biological samples could denature and alter the original molecular distribution information.[14] Therefore, it is imperative to obtain the molecular map from the live syntrophic communities.

Our key hypothesis is that DIET occurs in the biointerphase between the two *Geobacter* populations resulting in the observed molecular differences between co-cultured aggregates and other forms of microbes. To validate this postulation, the System for Analysis at the Liquid Vacuum Interface (SALVI)[13, 15, 16] combined with ToF-SIMS developed in our group was applied in this study. In our previous work, the liquid SIMS capability to detect biomarkers was demonstrated.[16-18] In this work, we have applied *in vivo* molecular imaging in the anaerobic syntrophic communities for the first time. The SALVI microreactor not only provides a surface for biofilm initial attachment and space for growth (Fig. 1), but also permits *in situ* and *in vivo* molecular imaging of living cells using surface sensitive ToF-SIMS in vacuum. Once the silicon nitride (SiN) membrane was punched through by the Bi_3^+ cluster primary ion beam, high intensity (Fig.1f II) and high resolution (Fig.1f III) spectral data from the surface of biofilms were directly acquired in sequence.[19-22] Three dimensional (3D) images (Fig. 1g) from the high intensity data collection (Fig.1f II) give the molecular

distribution in depth. In addition to co-cultured aggregates, to provide a comprehensive study, co-culture planktonic cells, pure cultured DL1 biofilm, DL1 planktonic cells, GS15 biofilm, GS15 planktonic cells, and uninoculated media were included in the sample matrix.

Unlike the bulk information obtained from LC-MS/MS or denatured structural information of dried samples acquired by traditional static SIMS, surface characteristic biological molecules from living cells were observed in this study, including amino acids, lipids, polymers, and water clusters. Spectral Principal Component Analysis (PCA) was conducted with selected peaks that derived from spectral overlay.[23] Aromatic amino acids and polymers relevant to electrical conductance were revealed to be more abundant in co-culture aggregates, indicating DIET was more prevalent in the interface of the dense syntrophic communities. In addition, phosphatidylethanolamines (PEs) relevant fragments were observed with higher abundance in co-culture aggregates. PEs are essential in cell attachment and may favor aggregation. Large water clusters were identified as a distinguishing characteristic of co-cultured aggregates and planktonic cells in comparison with pure cultured biofilms and planktonic cells. Additionally, co-cultured aggregates differentiated from planktonic co-cultures by having slightly higher large water clusters, implying enhanced hydrophobic surface properties. The compositional changes in the co-cultured aggregates layers were captured by reconstructing the spectra along liquid SIMS dynamic depth profiling.

This work provides the first molecular mapping of the biointerface that is critical in DIET of the *Geobacter* co-culture system compared to previous works.[6-10] In situ liquid ToF-SIMS is a powerful surface characterization technique and it offers high resolution chemical mapping, providing a new avenue for us to probe intercellular electron transfer. This is not possible using bulk techniques such as LC-MS/MS. The latter would be useful to obtain more complex omics information. Spectral PCA was used as an effective tool to differentiate a set of relevant samples to mine crucial understanding.[24] Specifically, we focus on the top surface of the co-cultured aggregates and evaluate the role of DIET in a living system using in vivo molecular imaging. The unique molecular composition of co-cultured aggregates is revealed in nature, which improves our understanding of the electron transfer mechanism of how syntrophic communities evolved and developed.

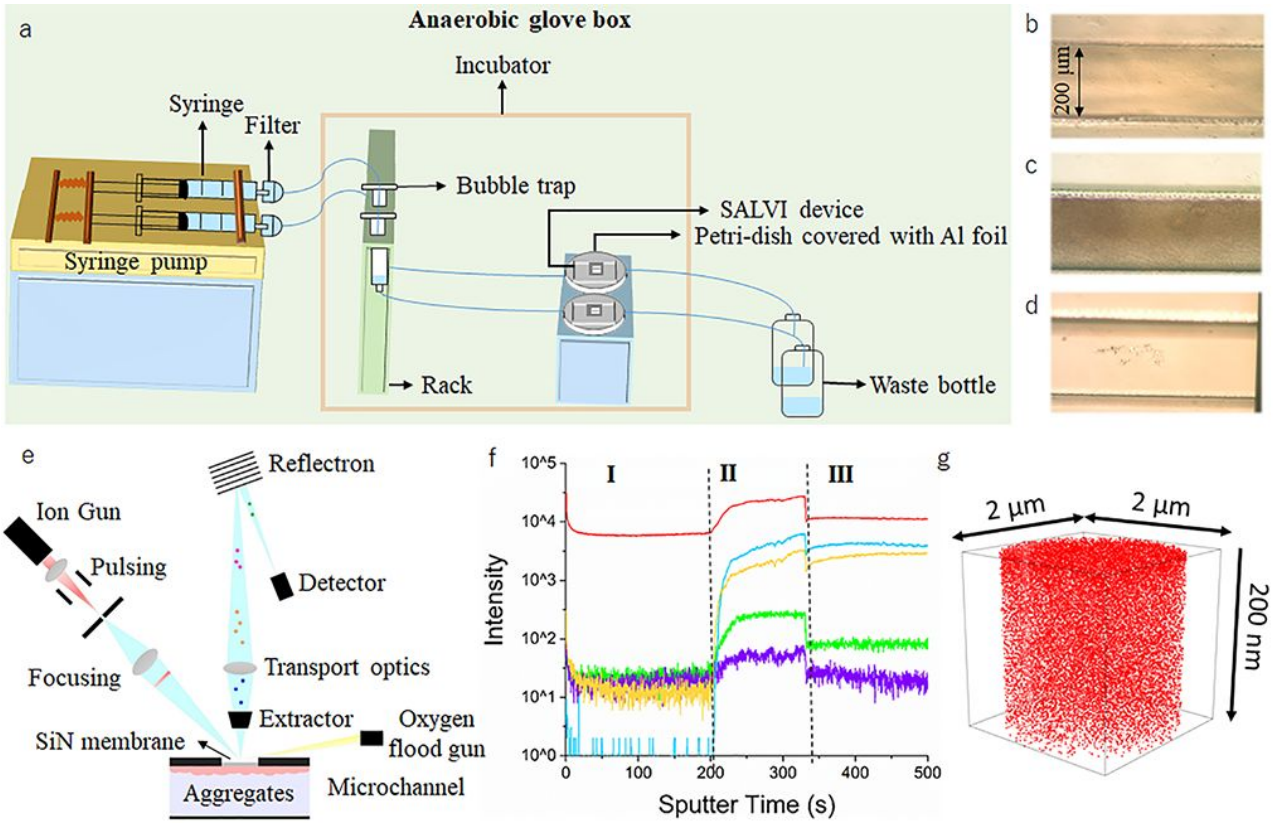

Figure 1. (a) Schematic of microbial cultivation. Optical images of (b) pure cultured *G. sulfurreducens* biofilm, (c) pure cultured *G. metallireducens* biofilm, and (d) co-cultured aggregates formed by the two *Geobacter* species within the SALVI channel. (e) *In situ* liquid SIMS schematic; (f) dynamic depth profiling of *Geobacter* co-cultures; and (g) representative superimposed 3D images acquired from (f).

Experimental

Fabrication of SALVI

Details of SALVI fabrication were described in our previous studies.[13, 16] The SALVI device enables liquid analysis using traditional surface vacuum instruments. The key design was a microchannel, which was embedded in a polydimethylsiloxane (PDMS) block by soft lithography and enclosed by a 100-nm thick SiN membrane. The dimensions of the microchannel were 200 µm wide by 300 µm deep for biofilm culture.

Cultivation of co-culture aggregates

Active *Geobacter sulfurreducens* DL1 (ATCC 51573) and *Geobacter metallireducens* GS15 (ATCC 53774), both of which reached their log phase,[13] were inoculated with the volume ration of 1:1 in the SALVI device. After adequate initial attachment, continued fresh NB fumarate (NBF) medium with 10 mM ethanol added was provided by the syringe pump (Cole-Parmer) at the rate

of 4 μL/min. Strict anaerobic conditions with a constant temperature of 30 ℃ was maintained by using the anaerobic glove box (MBraun LAB master, 100% N_2, O_2 < 2.3 ppm) and incubator (10-140E, Quincy Lab). The experimental setup and workflow were depicted in Figs. 1 and S1. Pure cultured biofilms were prepared using the same platform. Once the matured biofilm was formed on the SiN window (Figs. 1 and S2), the SALVI device was detached from the platform, sealed by a PEEK union, then transferred into the chamber of ToF-SIMS by an anaerobic jar. Table S1 summarizes information on the cultivation of the biological samples including co-culture planktonic cells, pure co-cultured DL1 biofilms and planktonic cells, pure cultured GS15 biofilm, and its planktonic cells. More details were reported previously.[13]

ToF-SIMS

A ToF-SIMS V spectrometer (IONTOF GmbH, Münster, Germany) was employed for data acquisition. A 25 keV Bi_3^+ primary ion beam was used. We have demonstrated its application in studying biological and environmental interfaces using the in situ liquid ToF-SIMS approach. [18, 20-22] Recent results show that it offers soft ionization and ensures analysis of soft materials. Several previous efforts in single population living biofilm studies also show the potential of combining biofilm culture in a microfluidic reactor and in situ imaging using ToF-SIMS that is traditionally limited to solid samples.[16, 17, 25] During measurements, a 1 keV O_2^+ cluster beam was used for charge compensation with a filament current of 2.20 pA. A higher current of 150 ns pulse width was employed during depth profiling until 100 s after the punch-through of the SiN membrane and higher resolution data were obtained for image reconstruction. Then a lower current with 50 ns pulse width was employed for sputtering for another 200 s, and high mass resolution spectra were collected. ToF-SIMS data were collected in the mass range of 1-800. For each sample, 4 negative and 4 positive data points were gathered at different locations along the microchannel, which have shown good reproducibility (Figs. S3a-d). We have done DI water data collection extensively, and the precision remained consistent over 9 data points. The same was true with other biological samples.[26] The imaging area was 2.0 μm × 2.0 μm^2 in a random raster mode with 64 by 64 pixels. The liquid surface was held by surface tension to balance against the vacuum pressure during the in the in situ liquid SIMS analysis.[16, 17, 27, 28] The *Geobacter* aggregate community was cultured and safely protected in the microchannel of the SALVI device when it was brought for in situ liquid ToF-SIMS analysis. We have done similar experiments of other single population strain.[16-18] This has been the first laboratory effort to extend the technique to study co-cultures.

ToF-SIMS Data analysis

Peaks such as Si^-, SiO_2^-, PO_2^-, PO_3^-, $Si_2HO_5^-$, and $Si_3HO_7^-$ in the negative mode and Si^+, Bi^+, Bi_2^+, and Bi_3^+ in the positive mode, were used in mass calibration, respectively, in the IONTOF software (Surface Lab 6.4). In order to identify key components that differentiate co-culture aggregates from others, we performed PCA (Matlab, R2012a, MathWorks, Inc., MA) with different sets of peak selection. Prior to performing PCA, data were normalized to the selected total ion intensities, square root transformed, and meancentered.[17, 18] Considering the challenge of peak identification, we made efforts from four perspectives. Firstly, literatures were searched using similar static SIMS conditions (Tables S2-S5). Secondly, a parallel study was performed using dried samples to collect molecular information using static SIMS that have superior mass resolution compared to in situ liquid SIMS.[13] Thirdly, we did SIMS experiment with reference agents (Table S6). Lastly, additional instrument development efforts will be continued to enhance the mass resolution of in situ liquid SIMS.[22]

Atomic Force Microscopy (AFM)

An MFP-3D AFM (Asylum Research) instrument was employed to acquire AFM images. The experiment was performed at room temperature. Silicon cantilevers (SSS-NCL, Nano World) were used, which have a tip radius < 5 nm and a spring constant of ~ 48 N/m. In order to minimize damage to samples, low set point amplitudes (< 300 mV) was used while obtaining AFM images in the tapping mode. Igor Pro 6.34 software (WaveMetrics) was used in AFM mages analysis.

Results and Discussion

Due to the current limitation in liquid SIMS,[13, 22, 29] only unit mass accuracy is available. To facilitate peak identification, traditional static ToF-SIMS analysis of solid samples was used to obtain reference spectra with higher mass accuracy.[13] Moreover, a number of previous studies were referred to (Tables S2-5).[20, 22] To confirm peak identification of some key species, reference samples were analyzed (Table S6). Because of the unit mass nature of liquid SIMS,[22] undoubtedly improved mass resolution and mass accuracy are needed for more accurate peak identification. A number of developments in SIMS instrumentation may provide a solution to this challenge, including MS-MS SIMS[30] and 3D NanoSIMS molecular imaging.[31] In this paper, we focus on the new biofilm findings based on the microfluidic reactor SALVI and liquid ToF-SIMS as a platform available to most people currently.

Observation from SIMS spectra

In this work, additional ToF-SIMS spectra are depicted and compared in Figs. S4a-d. Despite some interference peaks derived from the medium, microfluidic device, and the primary ion beam, a series of biological relevant peaks (Tables S2 and S3) were observed in both negative and positive spectra. Specifically, strong signals were detected at m/z^+ 30 CH_4N^+, 44 $C_2H_6N^+$, and 70 $C_3H_4NO^+$, which were mostly likely amino acids peaks.[32-36] Additionally, many lipid/fatty-acid fragment peaks were observed, such as m/z^- 223 $C_{14}H_{23}O_2^-$ and 239 $C_{15}H_{27}O_2^-$.[17, 37-39] Moreover, other significant biological components, such as polymer peaks m/z^+ 51 ($C_4H_3^+$) and m/z^- 121 $C_7H_5O_2^-$,[40, 41] and DNA base peaks, such as m/z^- 110 $C_4H_4N_3O^-$ and 150 $C_5H_4N_5O^-$,[42, 43] were observed. Our results show that SALVI enables *in situ* molecular imaging of living microbial systems, even anaerobically. *In vivo* and *in situ* molecular characterization tools could fill the gap of traditional mass spectrometry and capture valuable information that is lost when drying or freezing biological samples.

Among the detected biological signals, we are most interested in those that differ between co-culture aggregates and other samples. Therefore, several rounds of PCA were conducted using the peak spectral overlay strategy for peak selection,[23] with the goal of removing the maximal numbers of interference peaks derived from two kinds of medium salts (Figs. S5a-d). When compared with all peak PCA, the medium effects were reduced in selected peak PCA.[23] Selected peak PCA in the positive and negation modes (Figs. 2, 3 and S6a-b) show that the co-culture aggregates differ from various control samples, including co-culture planktonic cells, pure cultured biofilms, pure cultured planktonic cells, and medium solutions, indicating that unique molecular composition was formed in this syntrophic communities. Combined with the respective loadings plots, peaks that account for those discriminations were revealed. We give more discussions in the following sections.

Denser aromatic components in co-culture aggregates

Pili have been identified as the third strategy of microbial extracellular electron transfer,[44] in addition to redox active c-type cytochromes and shuttling molecules.[9] The conductivity of *G.*

sulfurreducens pili was shown visually under electrostatic force microscopy (EFM).[10] Furthermore, the stacking of some key aromatic amino acids was speculated and shown to be responsible for the metallic-like conductivity of pili.[45-48] This was also supported by studies showing that once the key aromatic amino acids of *G. sulfurreducens* were substituted by non-aromatic ones in the designed strain Aro-5, the conductivity was decreased.[49 50] Furthermore, higher conductivity was observed in another designed strain MP, which contained the pilA gene from *G. metallireducens* and produced more pili that had greater abundance of aromatic amino acids.[46]

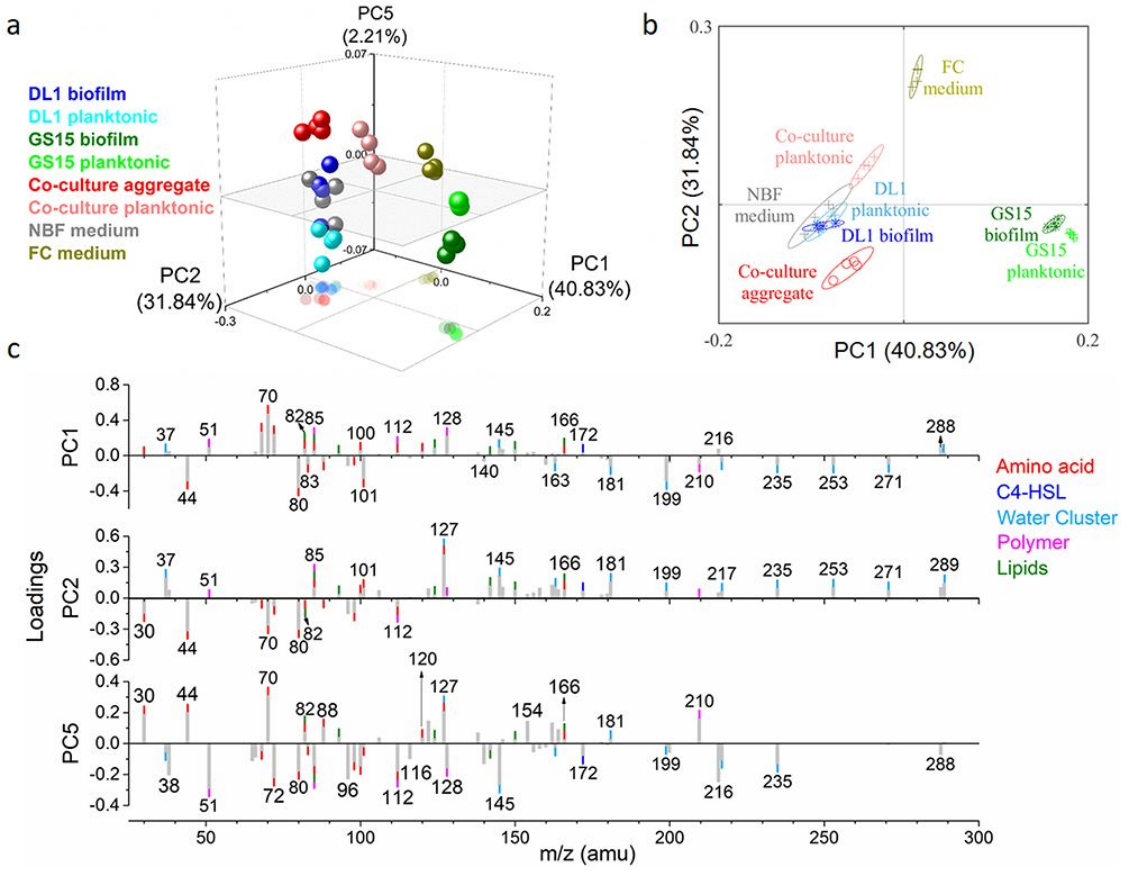

Figure 2. Selected peak spectral PCA in the positive mode. (a) 3D scores plots of PC1, PC2, and PC5; (b) PC1 vs. PC2 scores plot; and (c) loadings plots of PC1, PC2, and PC5. The shaded markers are the 3D reflection on the PC1 vs. PC2 plane. The ellipses represent 95% confidence intervals for each set of spectra.

Although the nature of electrically conductive pili was clearly demonstrated by EFM visually using the pure strain, we are more interested in the expression pattern in syntrophic cultures in this study. Some molecular methods, such as qPCR, could provide us with quantitative information on specific gene and protein expression levels. However, the obtained results are from the pool or ensemble, not from the contacting surface of the syntrophic community. Traditional mass spectrometry and electron microscopy could provide such information on the outer surface of the biointerphase; however, they require sample preparation via air drying, freezing, or staining treatments, which would kill the bacteria and denature the membranes.[14, 51] Therefore, the application of *in vivo* molecular imaging could compensate the shortage of traditional methods and provide molecular information on living syntrophic cultures.

Interestingly, ToF-SIMS spectral PCA results show that some aromatic amino acids, as fragments of proteins, played a role in differentiating the co-culture aggregates from the pure cultures, and even from co-culture planktonic cells. For example, in the positive PCA (Fig. 2), m/z$^+$ 82 ($C_4H_6N_2^+$, histidine),[36, 52-55] 120 ($C_8H_{10}N^+$, phenylalanine),[32-34, 56] and 166 ($C_9H_{12}NO_2^+$, phenylalanine)[54, 57, 58] were observed with positive loadings in PC5, all contributing to the separation of co-culture samples from others, especially for the co-culture aggregates. Previous studies showed enhanced density of aromatic amino acids, and the reduced gap between those compounds could lead to a significant increase of electrically conductivity of pili in the genetically modified *G. sulfurreducens*.[45, 46] The enhanced density of aromatic amino acids on the contacting surface of co-culture aggregates verifies the biological structure base of pili as the prevalent DIET pathway, which is evidenced by the high abundance of pili expressed. Additionally, it directly reveals the unique molecular structures formed when two *Geobacter* species form a co-culture.

Consistent with the findings obtained from the positive spectra, a series of fragments associated with benzene polymers were detected in the negative spectra, contributing to the distinction of co-culture aggregates and GS15 biofilms. For example, m/z$^-$ 93 $C_6H_5O^-$,[41] 94 $C_6H_6O^-$,[41] and 133 $C_9H_9O^-$ were observed with higher loadings in the positive PC2 in Fig. 3,[59] implying higher abundance in co-culture aggregates and GS15 biofilms. On the other hand, some non-aromatic polymers relevant to carbon bone chains were observed with prevalence in pure cultures, such as m/z$^+$ 51 $C_4H_3^+$ and 128 $C_{10}H_8^+$.[40] Serving as components in biological samples, polymers play a vital role in forming syntrophic associations. Due to the insufficient reference materials for identification of the source materials, it is difficult to determine if these benzene polymers are detached off those aromatic amino acids. Regardless, these benzene polymers probably play a similar role with aromatic

amino acids in long-distance electron transfer by forming pi-pi orbitals.[45] It is likely that the peak m/z$^+$ 51 could be assigned as a diagnostic fragment for benzene ring compounds due to the lower mass resolution nature of liquid SIMS. We propose the peak assignment to be $C_8H_{10}N^+$ as an aromatic amino acid phenylalanine fragment, because our previous work using high mass accuracy static ToF-SIMS provided additional support of this assignment.[13] Further, aromatic amino acids are known players of DIET. The higher occurrence of aromatic polymers in co-culture aggregates and GS15 biofilms is intriguing, because *G. matellireducens* was reported to have orders of magnitude higher conductivity than *G. sulfurreducens*,[46] probably owing to the higher abundance of aromatic amino acids. Our findings further support that opinion with the *in vivo* observation of denser aromatic polymers on the contacting surface of aggregates. Furthermore, these results suggest GS15, as the electron donor, play a more dominant role in the aggregated co-culture communities.

Enhanced PEs for aggregation

In addition to proteins and polymers, lipids are regarded as crucial components in the extracellular polymeric substance (EPS) of biofilms. However, only limited studies have focused on *Geobacter* lipids.[60, 61] Without complicated extracting procedures, characteristic fragments of lipids could be detected directly by *in vivo* liquid SIMS in this work. Lipids in different categories were captured, including fatty acids, glycerolipids, and a series of phospholipids.

It is worth noting that PE fragments were observed as a prime component that favored the distinction of co-culture aggregates from other samples, especially for the planktonic pure cultures (Fig. 3). For example, m/z$^-$ 196 ($C_5H_{11}NPO_5^-$, phosphatidylethanol-amine)[62] has higher loading in positive PC2, which contributes to the differentiation of co-culture aggregates and GS15 biofilms. m/z$^-$ 126 ($C_2H_9NPO_3^-$, 2-aminoethylphosphono lipids)[63] and 140 ($C_2H_7NPO_4^-$, phosphatidylethanol-amine)[62, 64, 65] have relatively smaller loadings in the negative PC5, which contribute to the differentiation of co-culture aggregates and DL1 biofilms. PEs serve as critical building stocks of membranes.[66] The overexpression of PEs in sessile microbial cells, compared with their planktonic counterparts, may serve to increase the stability of biofilms. This was consistent with observations from previous studies,[66, 67] showing the important role of PEs in reducing the fluidity of biofilms. Besides enhancing the biofilm stability, PEs were responsible for inter-lipid contacts via intermolecular H-bonding, such as generating structural intermediates.[68] This was especially interesting, as the surface cells play a key role in the exchange of nutrients, waste, or electrons for the whole syntrophic culture. The enhanced PE level in syntrophic aggregates implies the adaption of biological structures to the altered needs from the syntrophic culture.

Additionally, PC2 in the negative selected peak PCA in Fig. 3 shows that a series of fatty acid fragments, such as m/z$^-$ 237 ($C_{16}H_{29}O^-$),[17] 269 ($C_{17}H_{33}O_2^-$),[26] and 279 ($C_{18}H_{31}O_2^-$, linoleic acid),[17] are more abundant in co-culture planktonic cells, thus favoring the separation from aggregated co-cultures. Since little findings involving fatty acids have been reported in previous *Geobacter* studies, one possible explanation was that these increased fatty acids may alter the surface hydrophobic properties and make it more fluidic than aggregated communities. This finding needs further investigation.

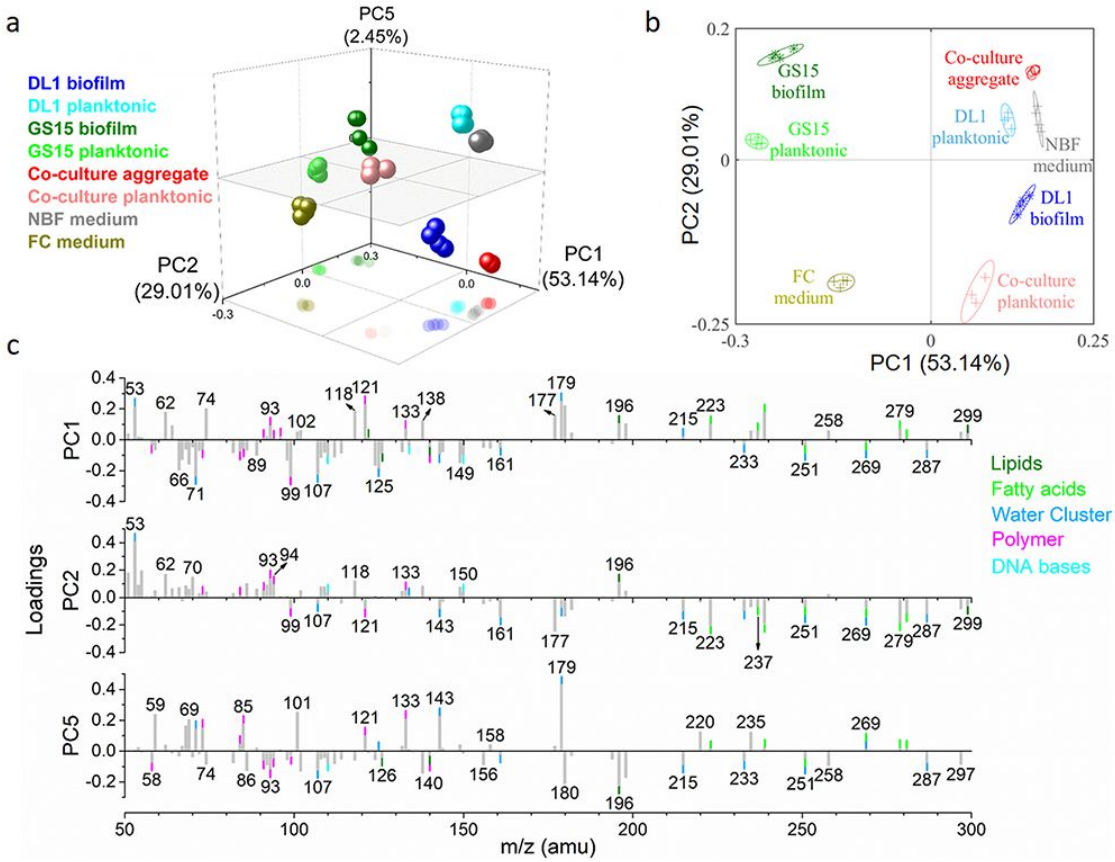

Figure 3. Selected peak spectral PCA in the negative mode. (a) 3D scores plots of PC1, PC2, and PC5; (b) PC1 vs. PC2 scores plot; and (c) loadings plots of PC1, PC2, and PC5. The shaded markers are the 3D reflection on the PC1 vs. PC2 plane. The ellipses represent 95% confidence intervals for each set of spectra.

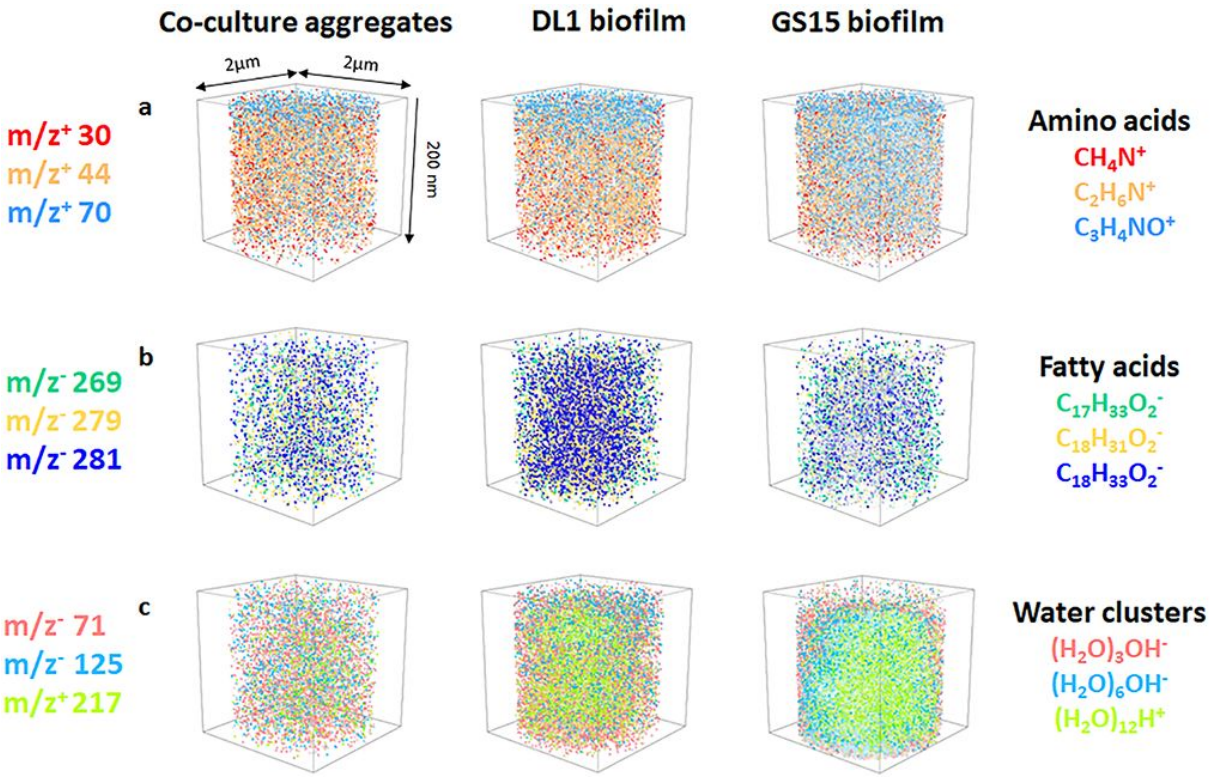

Figure 4. Normalized and superimposed 3D images of representative amino acids, fatty acids and water clusters observed in this study.

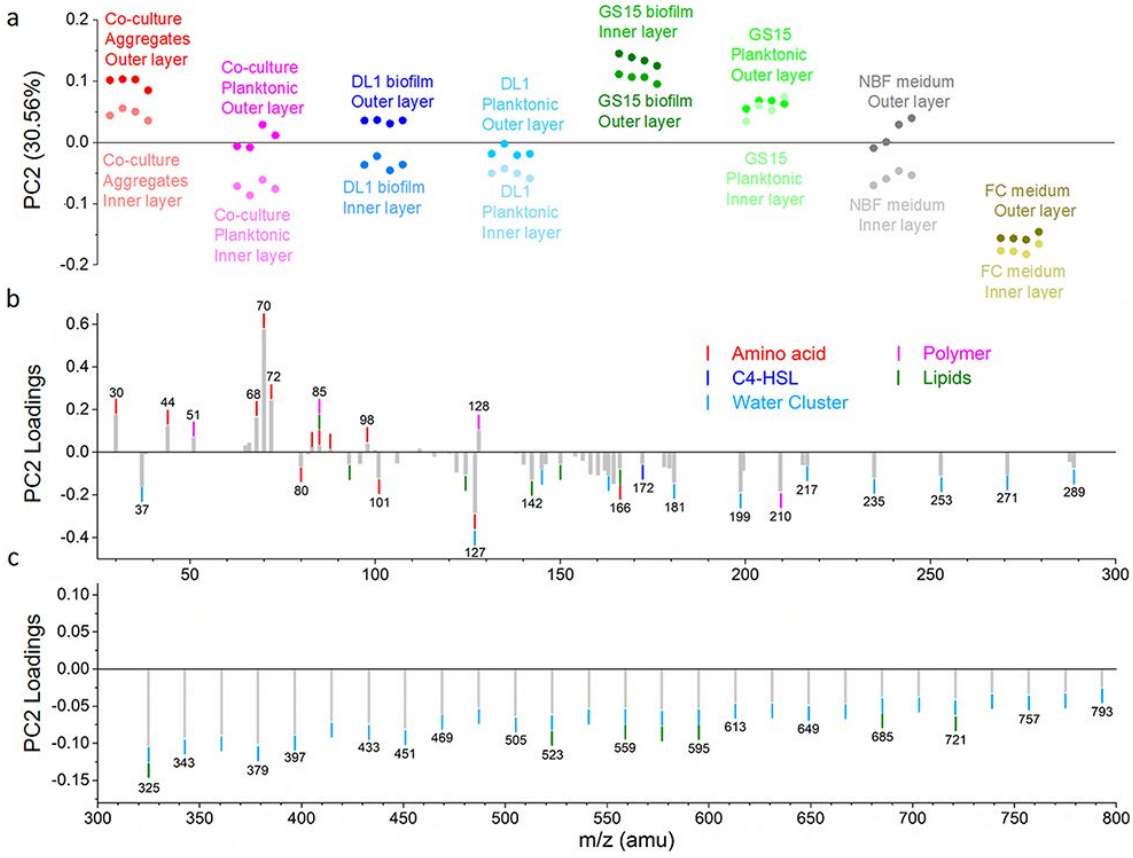

Figure 5. Representative scores and loadings plots of selected peak spectral PCA in the positive mode comparing the outer and inner layers. (a) Scores plot of PC2 and loadings plots of PC2 in the m/z range of 50-300 (b) and 300-800 (c), respectively.

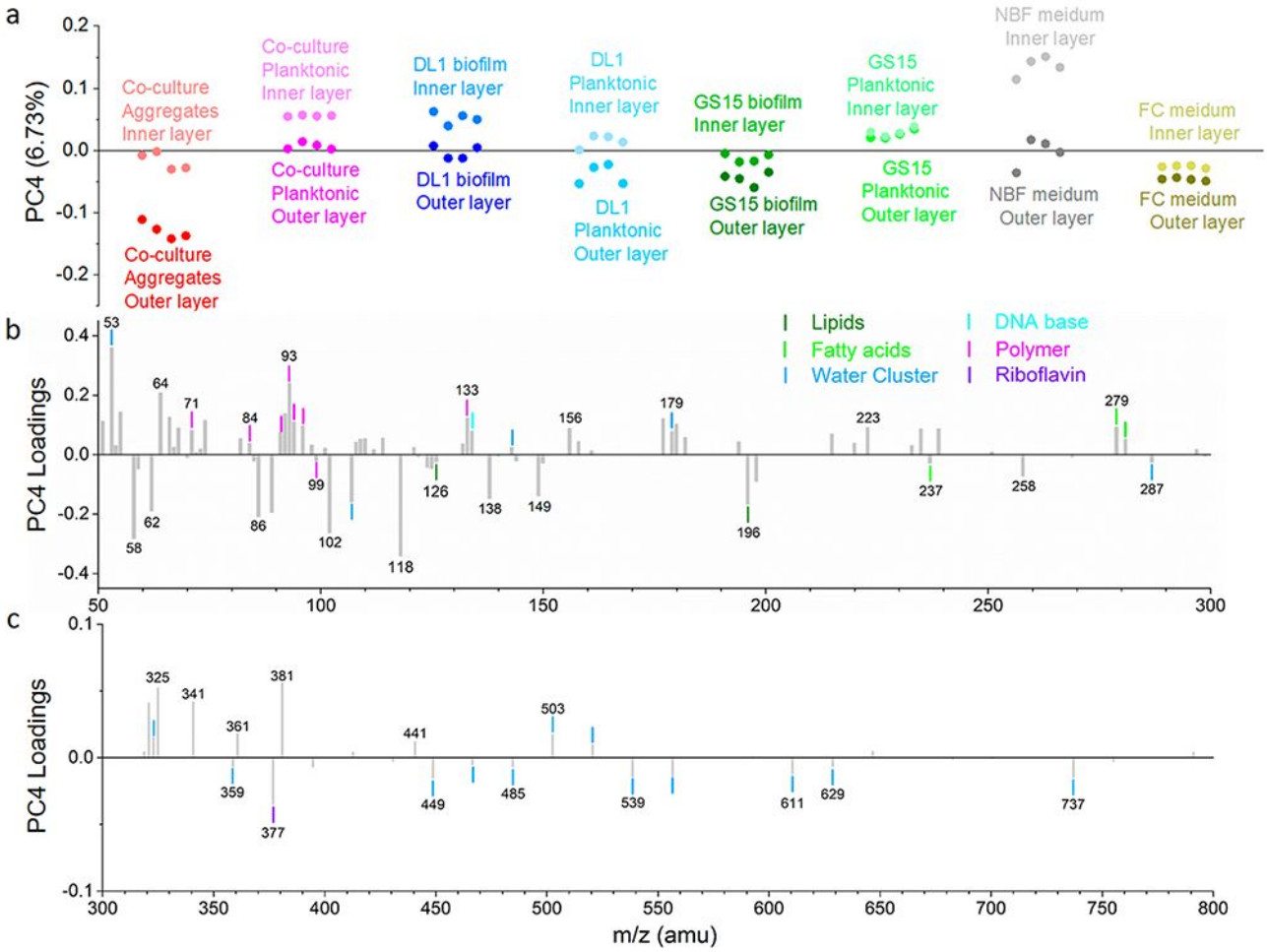

Figure 6. Representative scores and loadings plots of selected peak spectral PCA in the negative mode comparing the outer and inner layers. (a) Scores plot of PC4 and loadings plots of PC4 in the m/z range of 50-300 (b) and 300-800 (c), respectively.

Different distribution of water clusters

Water microenvironment plays an influential role in a series of biological functions of living organisms. However, information on the distribution of water clusters surrounding the living organisms is limited, due to the difficulty in using vacuum-based instruments to study liquids.[17] To fill this gap, a vacuum compatible microreactor or SALVI was invented and described in our previous studies.[13, 15, 28] We have first applied it in the anaerobic syntrophic system in this work. Using ToF-SIMS, substantial water clusters were observed, for example, m/z$^+$ 235 $(H_2O)_{13}H^+$, 343 $(H_2O)_{19}H^+$, 541 $(H_2O)_{30}H^+$ in the positive spectra (Table S4)[17, 69-71] and m/z$^-$ 179 $(H_2O)_9H^-$, 413 $(H_2O)_{22}H^-$, 557 $(H_2O)_{30}H^-$ in the negative spectra (Table S5).[10,57-59] Selected peak PCA results show that while small water clusters (n<16) bear no apparent differences in the distribution pattern, large water clusters have a clear trend. To be specific, in the positive spectral PCA results, more large water clusters $(H_2O)_nH^+$, n=18-21, 23-44 were observed with higher loadings in the positive PC5 (Fig. S6a), which contributed to the distinction of co-cultured samples from pure cultured samples. They also slightly separated co-culture aggregates from co-cultured planktonic cells. In the negative spectral PCA, similar result was obtained. Namely, more large water clusters $(H_2O)_nH^-$, n=16-17, 19, 21-35, 37-38, 40-43 were observed to have significant loadings in the negative PC5 (Fig. S6b), which favored the separation of co-cultured aggregates from co-cultured planktonic cells. The different distribution patterns of large water clusters indicted the changes of the liquid micro-environment with the syntrophic community. Knowing that the interaction would be more intense between syntrophic cultures than pure cultures, large water clusters may serve as a "bridge" to facilitate their exchanges of metabolites or electrons via hydrogen bonding and weak molecular interactions. A previous study showed that excess electrons tend to bind to the surface of the cluster, which is less stable than the bulk hydrated electron due to the relatively smaller vertical binding energy.[69] In this work, selected peak PCA results (Figs. 2 and 3) provide the direct evidence that more larger water clusters are observed on the biointerphase of co-culture aggregates, suggesting that the intermolecular hydrogen bonding could facilitate electron transfer between the different single populations and benefit the DIET pathway. Moreover, large water clusters are known to reflect higher hydrophobicity at the surface, which favors the aggregation or biofilm formation.[17] Whether surface water clusters could directly favor DIET deserves further investigation.

Molecular profile changes

The vertical molecular distribution of the aggregate biointerface were captured using depth profiling. Normalized 3D images (Figs. 4, S7, S8a-b, and S9a-b) were reconstructed from the high intensity depth profiling segment (Fig. 1f III). Mixing and diffusion is unavoidable in liquid. The concentration change due to liquid volatility and liquid diffusion was mathematically estimated to be 1.2 - 2.2 times different compared to the original solution in vacuum.[27, 28] However, the situation was less complicated when analyzing sticky soft materials like microbial biofilms. The sequential AFM measurements of agarose plate and biofilms in Figure S10 suggest that the ToF-SIMS profiling depth be ~ 200 nm after the in situ liquid ToF-SIMS analysis. As the distribution of some molecules shown in 3D image (Fig. 4) are not homogeneous, we speculated that molecular changes existed in depth. To

investigate the differences between the outer and inner layers, another batch of PCA (Figs. 5-6) was conducted. The first 50 data points after the SiN membrane was punched through were discarded due to the potential interference from the primary ion beam and SiN collisional interactions. The following 200 data points were divided equally into two parts and reconstructed, corresponding to the outer and inner layer of the aggregates, respectively. Spectral PCA (Figs. 5-6) was conducted using the same peak list that was used in analyzing the high intensity data. Interestingly, while no apparent differences between outer and inner layer within the same sample were discerned in the dominant PCs in the results, clear separations were obtained in other PCs. For example, in the scores plots of PC2 in the positive mode (Fig. 5), the outer layers of co-culture aggregates and GS15 biofilms are differentiated from their respective inner layers with the corresponding higher loadings from amino acid peaks, including m/z$^+$ 30 CH_4N^+, 44 $C_2H_6N^+$, 68 $C_4H_6N^+$, 70 $C_3H_4NO^+$, 72 $C_4H_{10}N^+$, and 98 $C_4H_4NO_2^+$, and polymer peaks, such as m/z$^+$ 51 $C_4H_3^+$ and 128 $C_{10}H_8^+$. The changes in amino acid composition suggests that the alteration of surface proteins is unique from its inner layers. Higher abundance of $C_xH_y^+$ polymers implies the backbone components of EPS are highly expressed on the outer surface of syntrophic communities, and that they help to stabilize individual cells. Because the same trend is observed in co-culture aggregates and GS15 biofilms, it is reasonable to postulate that GS15 plays a key role in the outer surface of the syntrophic aggregates, either in expanding its species abundance or expressing its unique molecules such as pili or cytochromes. Coincidently, recent findings report that the electron donor species play a more powerful role in the formation of syntrophic consortia and the DIET process;[72] and the conductive pili cannot be substituted by magnetite while the electron acceptor can.[73, 74] As it is known that the surface of communities plays an indispensable role in exchanging nutrients and interacting with its syntrophic species as an energy source, our findings directly display that a unique biological structures exist on the outer surface of the communities in their living state.

Additionally, while the outer and inner layers of other samples were not well differentiated, the ones of co-culture aggregates were significantly separated by PC4 in the negative spectral PCA (Fig. 6). The PE peaks, such as m/z$^-$ 126 $C_2H_9NPO_3^-$ (2-aminoethylphosphono lipids) and 196 $C_5H_{11}NPO_5^-$ (phosphatidylethanol-amine), as discussed earlier, are shown to have higher abundance in the outer layer, providing an evidence of their role in aggregation. Excitingly, m/z$^-$ 377 $C_{17}H_{21}N_4O_6^-$ riboflavin (see Table S6), an important electron shuttle in extracellular electron transfer, was observed with high abundance in the outer layers of syntrophic aggregates, suggesting its potential role in facilitating DIET. Coincidently, a recent study also points out that riboflavin can promote EET that works as bound redox cofactors for cytochromes.[75, 76] As biological structures are highly correlated with their functions, our new findings suggest the unique role of the outer layer of co-culture aggregates in stabilizing and recruiting individual cells.

These findings raise the question of how deep the dynamic depth profiling went during the detection with higher current (150 ns pulse width). Due to the limitation of direct measurement of biofilms and lack of simultaneous depth measurements in the existing ToF-SIMS instrument,[25] a subsequent experiment was conducted using agarose as a surrogate. The latter is as soft as biofilms, allowing accurate measurements using AFM. The AFM depth measurements determined that the depth would be 200 nm during the 100 s profiling (Fig. S10). As the single *Geobacter* bacteria is around 2 - 3 μm in length and 200 nm in width,[74] it means that the molecular results obtained in this work is almost one single layer of bacteria. This complimentary measurement demonstrates that the *in vivo* ToF-SIMS can be an effective tool in revealing unique molecular mapping on the outer surface of biofilms and syntrophic microbial communities.

Conclusions

The surface molecular distribution of syntrophic *Geobacter* aggregates has been captured in their living state for the first time in this work. We detected a series of biomarkers, such as amino acids, lipids, fatty acids, and polymers, as well as water clusters, demonstrating the successful application of liquid ToF-SIMS in an anaerobic culture system. Spectral PCA further determines the key components that differentiated syntrophic *Geobacter* aggregates from syntrophic planktonic cultures, pure cultured planktonic cells, and biofilms. Our results show that aromatic components are more abundant in syntrophic *Geobacter* aggregates compared to other controls. This finding implies DIET may be more prevalent in the aggregated syntrophic community based on *in vivo* and *in situ* imaging. We find that phosphatidylethanolamines components have higher abundance on the surface of syntrophic *Geobacter* aggregates and potentially favor the aggregation progress. Since few studies have focused on the role of *Geobacter* lipids,[60, 61] our finding opens a new window for further investigation of its function. Interestingly, large water clusters are enriched in syntrophic *Geobacter* aggregates, suggesting that more hydrophobic surface properties are formed. Whether this enhancement would favor DIET deserves further investigation. 3D molecular changes are successfully captured *in vivo*, and another batch of PCA was performed to compare the outer and inner layer to uncover the unique components that are specially located on the outer biointerphase of the aggregates. This work has provided the first *in vivo* and *in situ* molecular imaging for syntrophic *Geobacter* aggregates and demonstrated the potential advantage of liquid ToF-SIMS in systems biology studies.

ASSOCIATED CONTENT

Supporting Information

Additional experimental details, figures and tables are provided in the supporting information. This material is available free of charge via the Internet at http://pubs.acs.org.

AUTHOR INFORMATION

Corresponding Author

*E-mail: xiaoying.yu@pnnl.gov. Phone: 1-509-372-4524. E-mail: fhliu@yic.ac.cn. Phone: 86-0535-2109268.

Author Contributions

The authors declare no competing financial interests.

Notes

The authors declare no competing financial interests.

ACKNOWLEDGMENT

Dr. Xiao-Ying Yu thanks for the support from Pacific Northwest National Laboratory (PNNL) Earth and Biological Sciences Directorate (EBSD) mission seed Laboratory Directed Research and Development (LDRD). Prof. Fanghua Liu thanks Yantai Institute of Coastal Zone Research Chinese Academy of Sciences with the funding from National Natural Science Foundation of China (No. 91751112 and 41573071. The research was performed in the W. R. Wiley Environmental Molecular Sciences Laboratory (EMSL), a national scientific user facility via the general user proposals 49694 and 50569. Microbial culture was conducted in the Biological Sciences Facility at PNNL. We are grateful to Prof. Derek Lovley for providing *Geobacter metallireducens* and

Geobacter sulfurreducens strains. We thank Xiaofei Yu for technical assistance. Wenchao Wei thanks the PNNL Alternate Sponsored Fellowship (ASF) and Graduate Fellowship from University of Chinese Academy of Sciences for support. PNNL is operated by Battelle for the DOE under Contract DE-AC05-76RL01830.

Key Words

in vivo, SALVI, ToF-SIMS, syntrophic *Geobacter* aggregates, DIET, molecular distribution

REFERENCES

(1) Rotaru, A. E.; Shrestha, P. M.; Liu, F.; Markovaite, B.; Chen, S.; Nevin, K. P.; Lovley, D. R., Direct Interspecies Electron Transfer between Geobacter metallireducens and Methanosarcina barkeri. *Appl Environ Microb* **2014,** *80* (15), 4599-4605.

(2) Liu, F. H.; Rotaru, A. E.; Shrestha, P. M.; Malvankar, N. S.; Nevin, K. P.; Lovley, D. R., Promoting direct interspecies electron transfer with activated carbon. *Energ Environ Sci* **2012,** *5* (10), 8982-8989.

(3) Katoa, S.; Hashimoto, K.; Watanabea, K., Microbial interspecies electron transfer via electric currents through conductive minerals. *Proceedings of the National Academy of Sciences* **2012,** *109* (25), 10042-10046.

(4) Summers, Z. M.; Fogarty, H. E.; Leang, C.; Franks, A. E.; Malvankar, N. S.; Lovley, D. R., Direct Exchange of Electrons Within Aggregates of an Evolved Syntrophic Coculture of Anaerobic Bacteria. *Science* **2010,** *330* (6009), 1413-1415.

(5) Zheng, S.; Zhang, H.; Li, Y.; Zhang, H.; Wang, O.; Zhang, J.; Liu, F., Co-occurrence of Methanosarcina mazei and Geobacteraceae in an iron (III)-reducing enrichment culture. *Front Microbiol* **2015,** *6*, 941.

(6) Voordeckers, J. W.; Kim, B. C.; Izallalen, M.; Lovley, D. R., Role of Geobacter sulfurreducens Outer Surface c-Type Cytochromes in Reduction of Soil Humic Acid and Anthraquinone-2,6-Disulfonate. *Appl Environ Microb* **2010,** *76* (7), 2371-2375.

(7) Tremblay, P. L.; Summers, Z. M.; Glaven, R. H.; Nevin, K. P.; Zengler, K.; Barrett, C. L.; Qiu, Y.; Palsson, B. O.; Lovley, D. R., A c-type cytochrome and a transcriptional regulator responsible for enhanced extracellular electron transfer in Geobacter sulfurreducens revealed by adaptive evolution. *Environ Microbiol* **2011,** *13* (1), 13-23.

(8) Inoue, K.; Leang, C.; Franks, A. E.; Woodard, T. L.; Nevin, K. P.; Lovley, D. R., Specific localization of the c-type cytochrome OmcZ at the anode surface in current-producing biofilms of Geobacter sulfurreducens. *Env Microbiol Rep* **2011,** *3* (2), 211-217.

(9) Leang, C.; Qian, X. L.; Mester, T.; Lovley, D. R., Alignment of the c-Type Cytochrome OmcS along Pili of Geobacter sulfurreducens. *Appl Environ Microb* **2010,** *76* (12), 4080-4084.

(10) Malvankar, N. S.; Yalcin, S. E.; Tuominen, M. T.; Lovley, D. R., Visualization of charge propagation along individual pili proteins using ambient electrostatic force microscopy. *Nat Nanotechnol* **2014,** *9* (12), 1012-1017.

(11) Bansal, R.; Liermann, L. J.; Stanley, B. A.; Brantley, S. L.; Tien, M., Characterization and Proteomic Analysis ofGeobacter sulfurreducensPCA under Long-Term Electron-Donor Starvation. *Geomicrobiology Journal* **2015,** 00-00.

(12) Lebedev, N.; Stroud, R. M.; Yates, M. D.; Tender, L. M., Spatially Resolved Chemical Analysis of Geobacter sulfurreducens Cell Surface. *ACS Nano* **2019,** *13* (4), 4834-4842.

(13) Wei, W.; Zhang, Y.; Komorek, R.; Plymale, A.; Yu, R.; Wang, B.; Zhu, Z.; Liu, F.; Yu, X. Y., Characterization of syntrophic Geobacter communities using ToF-SIMS. *Biointerphases* **2017,** *12* (5), 05G601.

(14) Dohnalkova, A. C.; Marshall, M. J.; Arey, B. W.; Williams, K. H.; Buck, E. C.; Fredrickson, J. K., Imaging hydrated microbial extracellular polymers: comparative analysis by electron microscopy. *Appl Environ Microbiol* **2011,** *77* (4), 1254-62.

(15) Yang, L.; Zhu, Z.; Yu, X.-Y.; Thevuthasan, S.; Cowin, J. P., Performance of a microfluidic device for in situ ToF-SIMS analysis of selected organic molecules at aqueous surfaces. *Analytical Methods* **2013,** *5* (10), 2515.

(16) Hua, X.; Yu, X. Y.; Wang, Z.; Yang, L.; Liu, B.; Zhu, Z.; Tucker, A. E.; Chrisler, W. B.; Hill, E. A.; Thevuthasan, T.; Lin, Y.; Liu, S.; Marshall, M. J., In situ molecular imaging of a hydrated biofilm in a microfluidic reactor by ToF-SIMS. *Analyst* **2014,** *139* (7), 1609-13.

(17) Ding, Y.; Zhou, Y.; Yao, J.; Szymanski, C.; Fredrickson, J. K.; Shi, L.; Cao, B.; Zhu, Z.; Yu, X. Y., In Situ Molecular Imaging of the Biofilm and Its Matrix. *Anal Chem* **2016,** *88* (22), 11244-11252.

(18) Ding, Y.; Zhou, Y.; Yao, J.; Xiong, Y.; Zhu, Z.; Yu, X. Y., Molecular evidence of a toxic effect on a biofilm and its matrix. *Analyst* **2019,** *144* (8), 2498-2503.

(19) Yu, J. C.; Zhou, Y. F.; Hua, X.; Zhu, Z. H.; Yu, X. Y., In Situ Characterization of Hydrated Proteins in Water by SALVI and ToF-SIMS. *Jove-J Vis Exp* **2016,** *15* (108), 53708.

(20) Lam, S. Y.; Yu, J.; Wong, S. H.; Peppelenbosch, M. P.; Fuhler, G. M., The gastrointestinal microbiota and its role in oncogenesis. *Best Practice & Research Clinical Gastroenterology* **2017,** *31* (6), 607-618.

(21) Zhang, Y.; Zeng, W.; Huang, L.; Liu, W.; Jia, E.; Zhao, Y.; Wang, F.; Zhu, Z., In Situ Liquid Secondary Ion Mass Spectrometry: A Surprisingly Soft Ionization Process for Investigation of Halide Ion Hydration. *Anal Chem* **2019,** *91* (11), 7039-7046.

(22) Zhou, Y.; Yao, J.; Ding, Y.; Yu, J.; Hua, X.; Evans, J. E.; Yu, X.; Lao, D. B.; Heldebrant, D. J.; Nune, S. K.; Cao, B.; Bowden, M. E.; Yu, X.-Y.; Wang, X.-L.; Zhu, Z., Improving the Molecular Ion Signal Intensity for In Situ Liquid SIMS Analysis. *Journal of The American Society for Mass Spectrometry* **2016,** *27* (12), 2006-2013.

(23) Yang, C.; Wei, W.; Liu, F.; Yu, X. Y., Peak selection matters in principal component analysis: A case study of syntrophic microbes. *Biointerphases* **2019,** *14* (5), 051004.

(24) Graham, D. J.; Castner, D. G., Multivariate analysis of ToF-SIMS data from multicomponent systems: the why, when, and how. *Biointerphases* **2012,** *7* (1-4), 49.

(25) Hua, X.; Marshall, M. J.; Xiong, Y.; Ma, X.; Zhou, Y.; Tucker, A. E.; Zhu, Z.; Liu, S.; Yu, X. Y., Two-dimensional and three-dimensional dynamic imaging of live biofilms in a microchannel by time-of-flight secondary ion mass spectrometry. *Biomicrofluidics* **2015,** *9* (3), 031101.

(26) Yu, J.; Zhou, Y.; Engelhard, M.; Zhang, Y.; Son, J.; Liu, S.; Zhu, Z.; Yu, X.-Y., In situ molecular imaging of adsorbed protein films in water indicating hydrophobicity and hydrophilicity. *Scientific Reports* **2020,** *10*, 3695.

(27) Yang, L.; Yu, X.-Y.; Zhu, Z.; Thevuthasan, T.; Cowin, J. P., Making a hybrid microfluidic platform compatible for in situ imaging by vacuum-based techniques. *Journal of Vacuum Science & Technology A: Vacuum, Surfaces, and Films* **2011,** *29* (6), 061101.

(28) Yang, L.; Yu, X. Y.; Zhu, Z.; Iedema, M. J.; Cowin, J. P., Probing liquid surfaces under vacuum using SEM and ToF-SIMS. *Lab Chip* **2011,** *11* (15), 2481-4.

(29) Graham, D. J.; Wagner, M. S.; Castner, D. G., Information from complexity: Challenges of TOF-SIMS data interpretation. *Appl. Surf. Sci.* **2006,** *252* (19), 6860-6868.

(30) Fisher, G. L.; Bruinen, A. L.; Ogrinc Potočnik, N.; Hammond, J. S.; Bryan, S. R.; Larson, P. E.; Heeren, R. M. A., A New Method and Mass Spectrometer Design for TOF-SIMS Parallel Imaging MS/MS. *Analytical Chemistry* **2016,** *88* (12), 6433-6440.

(31) Fletcher, J. S.; Lockyer, N. P.; Vaidyanathan, S.; Vickerman, J. C., TOF-SIMS 3D Biomolecular Imaging of Xenopus laevis Oocytes Using Buckminsterfullerene (C60) Primary Ions. *Analytical Chemistry* **2007,** *79* (6), 2199-2206.

(32) Bernsmann, F.; Lawrence, N.; Hannig, M.; Ziegler, C.; Gnaser, H., Protein films adsorbed on experimental dental materials: ToF-SIMS with multivariate data analysis. *Anal Bioanal Chem* **2008,** *391* (2), 545-54.

(33) Baugh, L.; Weidner, T.; Baio, J. E.; Nguyen, P. C.; Gamble, L. J.; Stayton, P. S.; Castner, D. G., Probing the orientation of surface-immobilized protein G B1 using ToF-SIMS, sum frequency generation, and NEXAFS spectroscopy. *Langmuir* **2010,** *26* (21), 16434-41.

(34) Kempson, I. M.; Martin, A. L.; Denman, J. A.; French, P. W.; Prestidge, C. A.; Barnes, T. J., Detecting the Presence of Denatured Human Serum Albumin in an Adsorbed Protein Monolayer Using TOF-SIMS. *Langmuir* **2010,** *26* (14), 12075-12080.

(35) Lebec, V.; Boujday, S.; Poleunis, C.; Pradier, C. M.; Delcorte, A., Time-of-Flight Secondary Ion Mass Spectrometry Investigation of the Orientation of Adsorbed Antibodies on SAMs Correlated to Biorecognition Tests. *J Phys Chem C* **2014,** *118* (4), 2085-2092.

(36) Xia, N.; May, C. J.; McArthur, S. L.; Castner, D. G., Time-of-flight secondary ion mass spectrometry analysis of conformational changes in adsorbed protein films. *Langmuir* **2002,** *18* (10), 4090-4097.

(37) Touboul, D.; Brunelle, A.; Halgand, F.; De La Porte, S.; Laprevote, O., Lipid imaging by gold cluster time-of-flight secondary ion mass spectrometry: application to Duchenne muscular dystrophy. *J Lipid Res* **2005,** *46* (7), 1388-95.

(38) Mas, S.; Touboul, D.; Brunelle, A.; Aragoncillo, P.; Egido, J.; Laprevote, O.; Vivanco, F., Lipid cartography of atherosclerotic plaque by cluster-TOF-SIMS imaging. *Analyst* **2007,** *132* (1), 24-6.

(39) Leefmann, T.; Heim, C.; Kryvenda, A.; Siljestrom, S.; Sjovall, P.; Thiel, V., Biomarker imaging of single diatom cells in a microbial mat using time-of-flight secondary ion mass spectrometry (ToF-SIMS). *Org Geochem* **2013,** *57*, 23-33.

(40) Lau, Y. T. R.; Weng, L. T.; Ng, K. M.; Chan, C. M., Development of chain-folding of semicrystalline polymers in thin films: a combined ToF-SIMS and PCA analysis. *Surf Interface Anal* **2011,** *43* (1-2), 340-343.

(41) Hook, A. L.; Scurr, D. J., ToF-SIMS analysis of a polymer microarray composed of poly(meth)acrylates with C6 derivative pendant groups. *Surf Interface Anal* **2016,** *48* (4), 226-236.

(42) Lee, C. Y.; Harbers, G. M.; Grainger, D. W.; Gamble, L. J.; Castner, D. G., Fluorescence, XPS, and TOF-SIMS surface chemical state image analysis of DNA microarrays. *J Am Chem Soc* **2007,** *129* (30), 9429-9438.

(43) Arlinghaus, H. F.; Ostrop, M.; Friedrichs, O.; Feldner, J.; Gunst, U.; Lipinsky, D., DNA sequencing with ToF-SIMS. *Surf Interface Anal* **2002,** *34* (1), 35-39.

(44) Reguera, G.; McCarthy, K. D.; Mehta, T.; Nicoll, J. S.; Tuominen, M. T.; Lovley, D. R., Extracellular electron transfer via microbial nanowires. *Nature* **2005,** *435* (7045), 1098-1101.

(45) Vargas, M.; Malvankar, N. S.; Tremblay, P. L.; Leang, C.; Smith, J. A.; Patel, P.; Synoeyenbos-West, O.; Nevin, K. P.; Lovley, D. R., Aromatic Amino Acids Required for Pili Conductivity and Long-Range Extracellular Electron Transport in Geobacter sulfurreducens. *Mbio* **2013,** *4* (2), e00105-13.

(46) Tan, Y.; Adhikari, R. Y.; Malvankar, N. S.; Ward, J. E.; Woodard, T. L.; Nevin, K. P.; Lovley, D. R., Expressing the Geobacter metallireducens PilA in Geobacter sulfurreducens Yields Pili with Exceptional Conductivity. *Mbio* **2017,** *8* (1), e02203-16.

(47) Sun, Y. L.; Tang, H. Y.; Ribbe, A.; Duzhko, V.; Woodard, T. L.; Ward, J. E.; Bai, Y.; Nevin, K. P.; Nonnenmann, S. S.; Russell, T.; Emrick, T.; Lovley, D. R., Conductive Composite Materials Fabricated from Microbially Produced Protein Nanowires. *Small* **2018**, e1802624.

(48) Ru, X.; Zhang, P.; Beratan, D. N., Assessing Possible Mechanisms of Micrometer-Scale Electron Transfer in Heme-Free Geobacter sulfurreducens Pili. *J Phys Chem B* **2019,** *123* (24), 5035-5047.

(49) Ueki, T.; Nevin, K. P.; Rotaru, A. E.; Wang, L. Y.; Ward, J. E.; Woodard, T. L.; Lovley, D. R., Geobacter Strains Expressing Poorly Conductive Pili Reveal Constraints on Direct Interspecies Electron Transfer Mechanisms. *Mbio* **2018,** *9* (4), e01273-18.

(50) Liu, X.; Tremblay, P. L.; Malvankar, N. S.; Nevin, K. P.; Lovley, D. R.; Vargas, M., A Geobacter sulfurreducens Strain Expressing Pseudomonas aeruginosa Type IV Pili Localizes OmcS on Pili but Is Deficient in Fe(III) Oxide Reduction and Current Production. *Appl Environ Microb* **2014,** *80* (3), 1219-1224.

(51) Hua, X.; Szymanski, C.; Wang, Z.; Zhou, Y.; Ma, X.; Yu, J.; Evans, J.; Orr, G.; Liu, S.; Zhu, Z.; Yu, X. Y., Chemical imaging of molecular changes in a hydrated single cell by dynamic secondary ion mass spectrometry and super-resolution microscopy. *Integr Biol (Camb)* **2016,** *8* (5), 635-44.

(52) Wagner, M. S.; McArthur, S. L.; Shen, M.; Horbett, T. A.; Castner, D. G., Limits of detection for time of flight secondary ion mass spectrometry (ToF-SIMS) and X-ray photoelectron spectroscopy (XPS): detection of low amounts of adsorbed protein. *J Biomater Sci Polym Ed* **2002,** *13* (4), 407-28.

(53) Lhoest, J. B.; Wagner, M. S.; Tidwell, C. D.; Castner, D. G., Characterization of adsorbed protein films by time of flight secondary ion mass spectrometry. *J Biomed Mater Res* **2001,** *57* (3), 432-440.

(54) Schaepe, K.; Kokesch-Himmelreich, J.; Rohnke, M.; Wagner, A. S.; Schaaf, T.; Wenisch, S.; Janek, J., Assessment of different sample preparation routes for mass spectrometric monitoring and imaging of lipids in bone cells via ToF-SIMS. *Biointerphases* **2015,** *10* (1), 019016.

(55) Tyler, B. J.; Bruening, C.; Rangaranjan, S.; Arlinghaus, H. F., TOF-SIMS imaging of adsorbed proteins on topographically complex surfaces with Bi-3(+) primary ions. *Biointerphases* **2011,** *6* (3), 135-141.

(56) Kim, Y. P.; Hong, M. Y.; Kim, J.; Oh, E.; Shon, H. K.; Moon, D. W.; Kim, H. S.; Lee, T. G., Quantitative analysis of surface-immobilized protein by TOF-SIMS: effects of protein orientation and trehalose additive. *Anal Chem* **2007,** *79* (4), 1377-85.

(57) Tian, H.; Fletcher, J. S.; Thuret, R.; Henderson, A.; Papalopulu, N.; Vickerman, J. C.; Lockyer, N. P., Spatiotemporal lipid profiling during early embryo development of Xenopus laevis using dynamic ToF-SIMS imaging. *J Lipid Res* **2014,** *55* (9), 1970-80.

(58) Desmet, T.; Poleunis, C.; Delcorte, A.; Dubruel, P., Double protein functionalized poly-epsilon-caprolactone surfaces: in depth ToF-SIMS and XPS characterization. *J Mater Sci-Mater M* **2012,** *23* (2), 293-305.

(59) Chan, C.-M.; Weng, L.-T.; Lau, Y.-T. R., Polymer surface structures determined using ToF-SIMS. *Reviews in Analytical Chemistry* **2014,** *33* (1), 11–30.

(60) Hartner, T.; Straub, K. L.; Kannenberg, E., Occurrence of hopanoid lipids in anaerobic Geobacter species. *FEMS Microbiol Lett* **2005,** *243* (1), 59-64.

(61) Hedrick, D. B.; Peacock, A. D.; Lovley, D. R.; Woodard, T. L.; Nevin, K. P.; Long, P. E.; White, D. C., Polar lipid fatty acids, LPS-hydroxy fatty acids, and respiratory quinones of three Geobacter strains, and variation with electron acceptor. *J Ind Microbiol Biot* **2009,** *36* (2), 205-209.

(62) Adams, K. J.; DeBord, J. D.; Fernandez-Lima, F., Lipid specific molecular ion emission as a function of the primary ion characteristics in TOF-SIMS. *J Vac Sci Technol B Nanotechnol Microelectron* **2016,** *34* (5), 051804.

(63) Passarelli, M. K.; Winograd, N., Lipid imaging with time-of-flight secondary ion mass spectrometry (ToF-SIMS). *Biochim Biophys Acta* **2011,** *1811* (11), 976-90.

(64) Brulet, M.; Seyer, A.; Edelman, A.; Brunelle, A.; Fritsch, J.; Ollero, M.; Laprevote, O., Lipid mapping of colonic mucosa by cluster TOF-SIMS imaging and multivariate analysis in cftr knockout mice. *J Lipid Res* **2010,** *51* (10), 3034-45.

(65) Amaya, K. R.; Sweedler, J. V.; Clayton, D. F., Small molecule analysis and imaging of fatty acids in the zebra finch song system using time-of-flight-secondary ion mass spectrometry. *J Neurochem* **2011,** *118* (4), 499-511.

(66) Favre, L.; Ortalo-Magne, A.; Pichereaux, C.; Gargaros, A.; Burlet-Schiltz, O.; Cotelle, V.; Culioli, G., Metabolome and proteome changes between biofilm and planktonic phenotypes of the marine bacterium Pseudoalteromonas lipolytica TC8. *Biofouling* **2018,** *34* (2), 132-148.

(67) Benamara, H.; Rihouey, C.; Jouenne, T.; Alexandre, S., Impact of the biofilm mode of growth on the inner membrane phospholipid composition and lipid domains in Pseudomonas aeruginosa. *Biochimica et Biophysica Acta (BBA) - Biomembranes* **2011,** *1808* (1), 98-105.

(68) Murzyn, K.; Rog, T.; Pasenkiewicz-Gierula, M., Phosphatidylethanolamine-phosphatidylglycerol bilayer as a model of the inner bacterial membrane. *Biophys J* **2005,** *88* (2), 1091-103.

(69) Verlet, J. R.; Bragg, A. E.; Kammrath, A.; Cheshnovsky, O.; Neumark, D. M., Observation of large water-cluster anions with surface-bound excess electrons. *Science* **2005,** *307* (5706), 93-6.

(70) Vaida, V., Perspective: Water cluster mediated atmospheric chemistry. *The Journal of Chemical Physics* **2011,** *135* (2), 020901.

(71) Sui, X.; Zhou, Y.; Zhang, F.; Chen, J.; Zhu, Z.; Yu, X. Y., Deciphering the aqueous chemistry of glyoxal oxidation with hydrogen peroxide using molecular imaging. *Phys Chem Chem Phys* **2017,** *19* (31), 20357-20366.

(72) Nagarajan, H.; Embree, M.; Rotaru, A. E.; Shrestha, P. M.; Feist, A. M.; Palsson, B. O.; Lovley, D. R.; Zengler, K., Characterization and modelling of interspecies electron transfer mechanisms and microbial community dynamics of a syntrophic association. *Nat Commun* **2013,** *4*, 2809.

(73) Wang, O.; Zheng, S.; Wang, B.; Wang, W.; Liu, F., Necessity of electrically conductive pili for methanogenesis with magnetite stimulation. *PeerJ* **2018,** *6*, e4541.

(74) Liu, F. H.; Rotaru, A. E.; Shrestha, P. M.; Malvankar, N. S.; Nevin, K. P.; Lovley, D. R., Magnetite compensates for the lack of a pilin-associated c-type cytochrome in extracellular electron exchange. *Environ Microbiol* **2015,** *17* (3), 648-655.

(75) Huang, L.; Tang, J.; Chen, M.; Liu, X.; Zhou, S., Two Modes of Riboflavin-Mediated Extracellular Electron Transfer in Geobacter uraniireducens. *Front Microbiol* **2018,** *9*, 2886.

(76) Huang, L.; Liu, X.; Ye, Y.; Chen, M.; Zhou, S., Evidence for the coexistence of direct and riboflavin-mediated interspecies electron transfer in Geobacter co-culture. *Environ Microbiol* **2019,** *22* (1), 243-254.

A graphic entry for the Table of Contents (TOC)

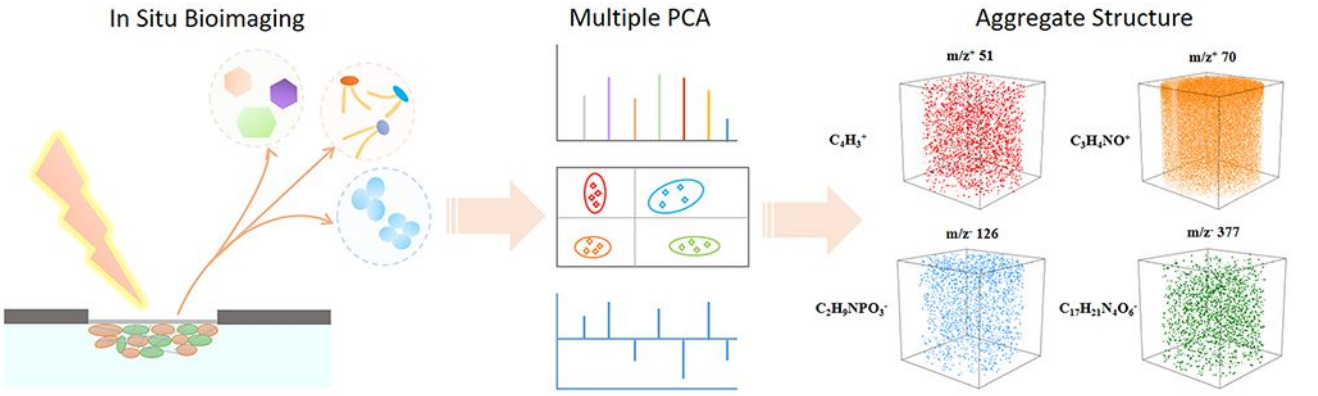

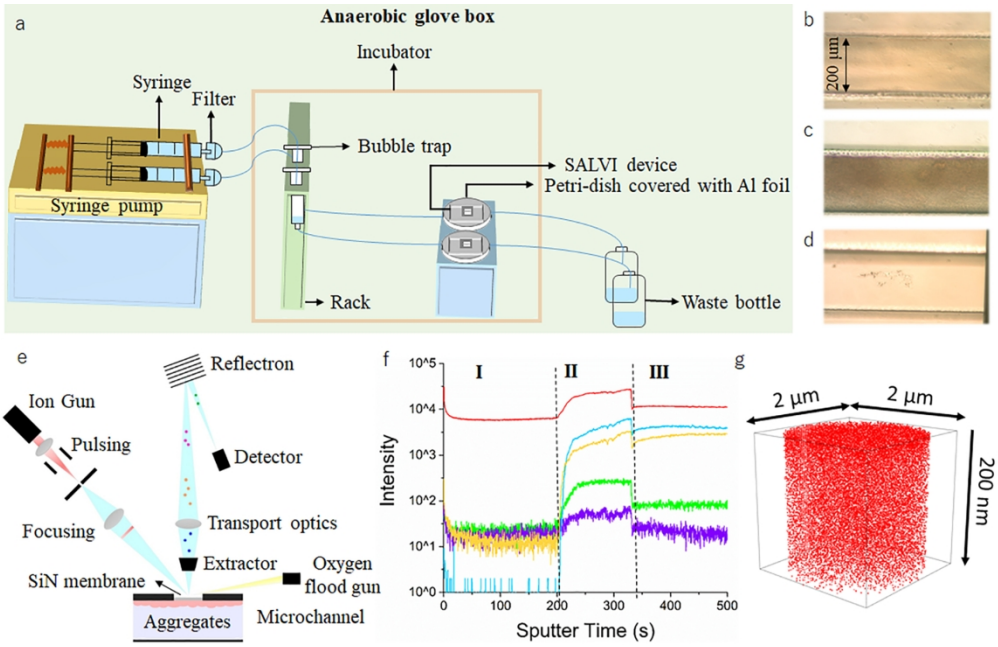

171x109mm (300 x 300 DPI)

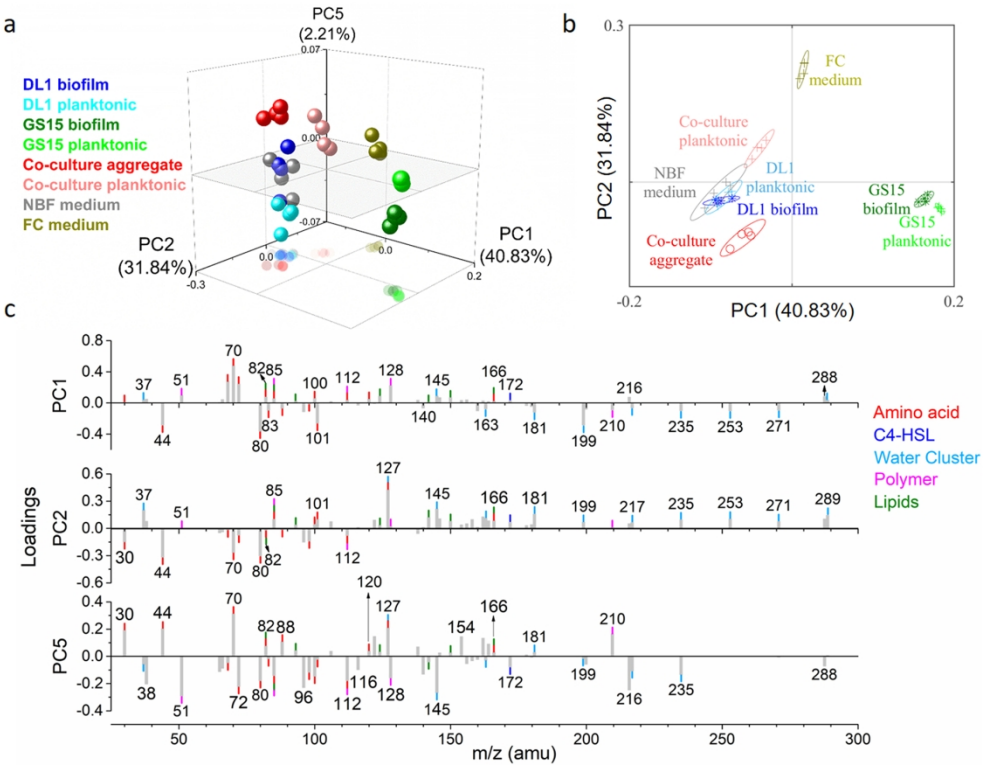
a
PC5 (2.21%)
PC2 (31.84%)
PC1 (40.83%)
DL1 biofilm
DL1 planktonic
GS15 biofilm
GS15 planktonic
Co-culture aggregate
Co-culture planktonic
NBF medium
FC medium
b
PC2 (31.84%)
PC1 (40.83%)
FC medium
Co-culture planktonic
NBF medium
DL1 planktonic
DL1 biofilm
GS15 biofilm
GS15 planktonic
Co-culture aggregate
c
Loadings
PC1
PC2
PC5
m/z (amu)
Amino acid
C4-HSL
Water Cluster
Polymer
Lipids

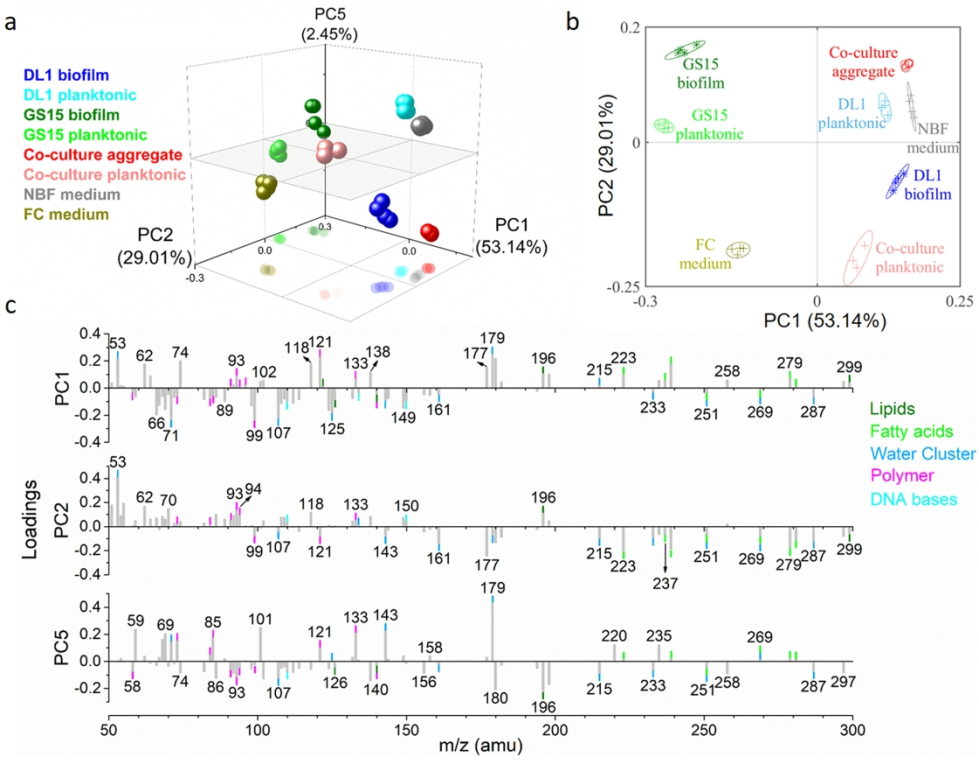
a
PC5
(2.45%)
DL1 biofilm
DL1 planktonic
GS15 biofilm
GS15 planktonic
Co-culture aggregate
Co-culture planktonic
NBF medium
FC medium
PC2
(29.01%)
PC1
(53.14%)
b
GS15
biofilm
Co-culture
aggregate
GS15
planktonic
DL1
planktonic
NBF
medium
DL1
biofilm
FC
medium
Co-culture
planktonic
PC2 (29.01%)
PC1 (53.14%)
c
Loadings
PC1
PC2
PC5
Lipids
Fatty acids
Water Cluster
Polymer
DNA bases
m/z (amu)

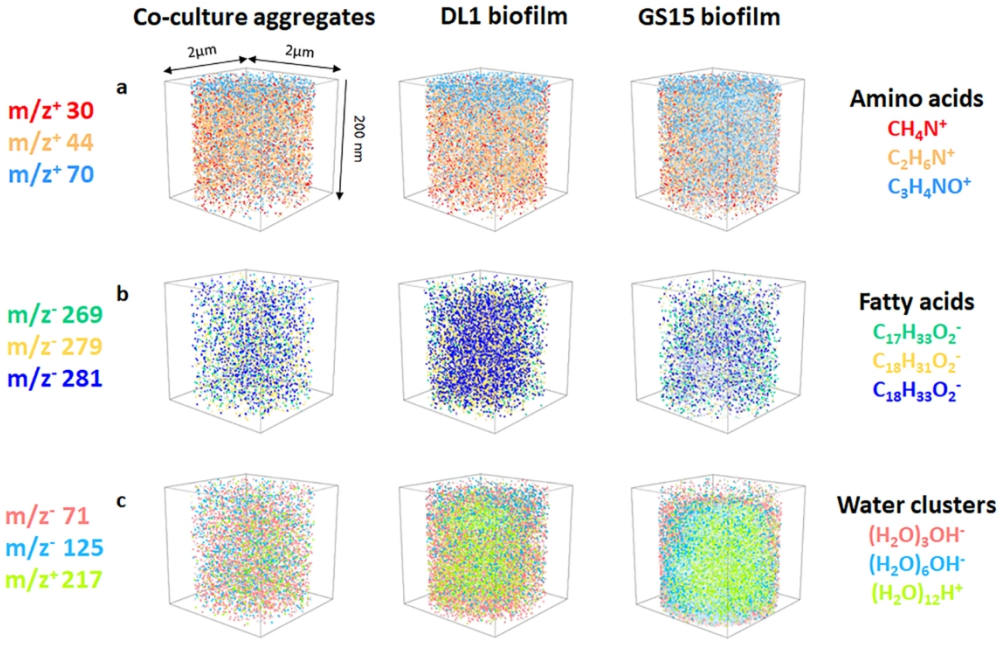

171x109mm (300 x 300 DPI)

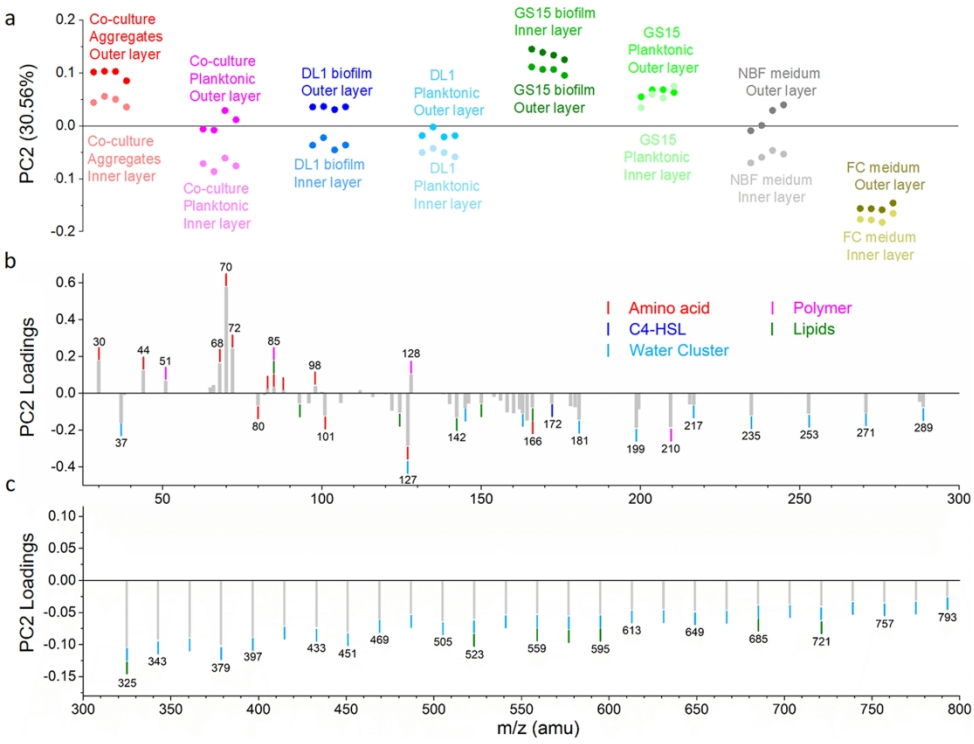
a
PC2 (30.56%)
Co-culture Aggregates Outer layer
Co-culture Aggregates Inner layer
Co-culture Planktonic Outer layer
Co-culture Planktonic Inner layer
DL1 biofilm Outer layer
DL1 biofilm Inner layer
DL1 Planktonic Outer layer
DL1 Planktonic Inner layer
GS15 biofilm Inner layer
GS15 biofilm Outer layer
GS15 Planktonic Outer layer
GS15 Planktonic Inner layer
NBF meidum Outer layer
NBF meidum Inner layer
FC meidum Outer layer
FC meidum Inner layer
b
PC2 Loadings
Amino acid
C4-HSL
Water Cluster
Polymer
Lipids
c
PC2 Loadings
m/z (amu)

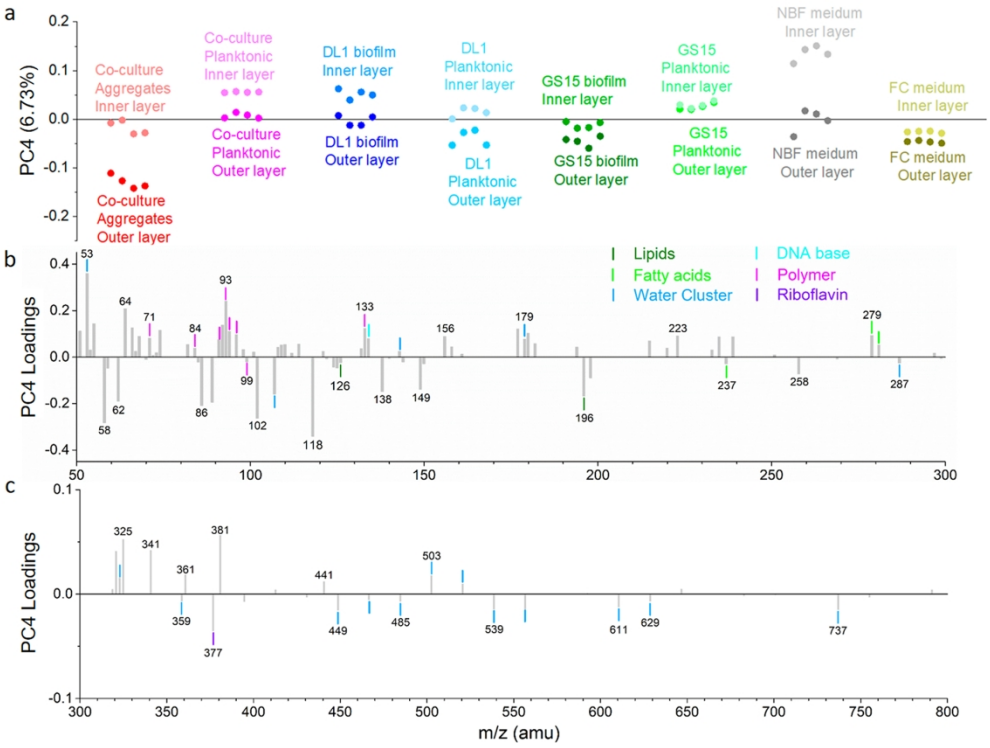
a
PC4 (6.73%)
Co-culture Aggregates Inner layer
Co-culture Aggregates Outer layer
Co-culture Planktonic Inner layer
Co-culture Planktonic Outer layer
DL1 biofilm Inner layer
DL1 biofilm Outer layer
DL1 Planktonic Inner layer
DL1 Planktonic Outer layer
GS15 biofilm Inner layer
GS15 biofilm Outer layer
GS15 Planktonic Inner layer
GS15 Planktonic Outer layer
NBF meidum Inner layer
NBF meidum Outer layer
FC meidum Inner layer
FC meidum Outer layer
b
PC4 Loadings
Lipids
Fatty acids
Water Cluster
DNA base
Polymer
Riboflavin
c
PC4 Loadings
m/z (amu)

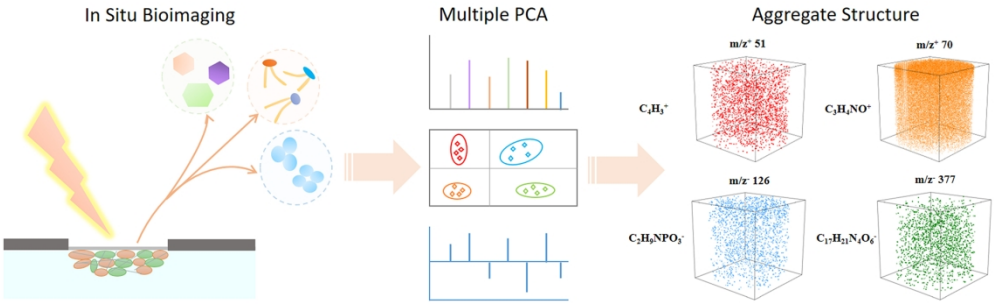
In Situ Bioimaging
Multiple PCA
Aggregate Structure
m/z+ 51
m/z+ 70
C4H3+
C3H4NO+
m/z- 126
m/z- 377
C2H9NPO3-
C17H21N4O6-